Materials Science Forum Vol. 590 (2008) pp 211-232
online at http://www.scientific.net

Nonpolar and Semipolar Orientations: Material Growth and Properties

Hisashi Masui[a] and Shuji Nakamura[b]

Solid-State Lighting and Energy Center, Materials Department,

College of Engineering, University of California, Santa Barbara

Santa Barbara, California 93106-5055 U.S.A.

[a]masui@engineering.ucsb.edu, [b]shuji@engineering.ucsb.edu

Keywords: wurtzite gallium nitride, nonpolar and semipolar orientations, lateral epitaxial overgrowth, threading dislocations, stacking faults

Abstract. Nitride-based optoelectronic devices prepared in the *c* orientation have been successfully introduced to the global marketplace and are changing the way we think about lighting. A part of the research interest has shifted toward nonpolar and semipolar orientations, which has the potential to broaden the scope and impact of this technology. This is because quantum-well structures prepared in nonpolar and semipolar orientations are able to suppress the quantum-confinement Stark effect, which has a negative impact on optoelectronic device performance. The lower crystal symmetry of such orientations provides spontaneously polarized light emission. Despite these attractive properties of nonpolar and semipolar orientations, the corresponding materials growth is not trivial. The present chapter discusses our efforts on growth of III-nitride materials in nonpolar and semipolar orientations and the related material properties.

Introduction

Group-III nitride compounds crystallize in the hexagonal wurtzite structure under common growth conditions. This chapter focuses on planar substrate and device structure growth on orientations other than the basal plane.

Early nitride growths for optoelectronic device applications such as light-emitting diodes (LEDs) were performed on the *c*-plane (basal plane). This was probably because the easy availability of *c*-plane sapphire substrates, which have advantages of stability at the nitride growth temperatures, high crystal quality, high transparency to the nitride emission range, large area, and low cost. The principal growth technique at those times was the metalorganic chemical vapor deposition (MOCVD) method, which commonly grows GaN crystals in the Ga-face direction $\langle 0001 \rangle$. This growth polarity along the c-axis was of interest for applications in LEDs, and several growth phenomena [1], such as substrate nitridation, inverted domains in Mg doping, and N-face growth in molecular beam epitaxy (MBE) were studied, however sidefaces and inclined facets did not call much attention.

Realization of InGaN-based laser diodes (LDs) was reported in 1996 [2]. Film growths in the nonpolar orientation were reported in 1996 with specific interest for laser devices [3]. About the same time, the quantum-confined Stark effect (QCSE) was discussed on quantum-well (QW) structures prepared on the *c*-plane [4]. QCSE is believed to have negative effects on optoelectronic devices via spatial separation of electrons and holes in QWs. Consequently, nonpolar orientations attract attention because of their potential to eliminate the QCSE. Indeed, such elimination of the QCSE has been demonstrated [5].

Device orientations other than the basal and nonpolar planes were implied by Park in 1999 [6]. Takeuchi et al. calculated effects on InGaN/GaN QWs of such orientations [7]. These planes were called semipolar planes by Baker et al. upon their success of planar film growth [8].

Nitride films were prepared via direct growth (either with or without nucleation layers, the latter is sometimes referred to as the two-step growth) onto foreign substrates. High defect densities were inevitable due to the direct growth until the lateral epitaxial overgrowth (LEO) technique was introduced in 1997 [9]. LEO and related techniques contributed to reduce the defect densities significantly in *c*-plane films grown on foreign substrates.

In 2006, sliced bulk-GaN substrates became commercially available in preferred orientations. Due to the excellent quality of those sliced bulk-GaN substrates, optoelectronic devices have recently experienced enormous developments in a short period of time.

Growth of Thick Films for Device Substrate Purposes

Planar growths of thick GaN films on foreign substrates have been performed for template purposes. Although the recent trend of device growths is the use of sliced bulk-GaN substrates, GaN films via hetero-epitaxial techniques are demanded for large area and potential cost efficiency. LEO is believed to be effective in such hetero-epitaxy. Crystals other than binary GaN have been only little explored.

Below is a list of combinations of GaN and substrate orientations.

a $(11\bar{2}0)$ GaN on *r* $(10\bar{1}2)$ sapphire and on *a* $(11\bar{2}0)$ SiC
m $(10\bar{1}0)$ GaN on *m* $(10\bar{1}0)$ SiC and on (100) γ-$LiAlO_2$
$(10\bar{1}\bar{1})$ GaN on (100) spinel ($MgAl_2O_4$)
$(10\bar{1}\bar{3})$ GaN on *m* $(10\bar{1}0)$ sapphire and on (110) spinel
$(11\bar{2}\bar{2})$ GaN on *m* $(10\bar{1}0)$ sapphire

Nonpolar Orientations. The *a* and *m* planes are the major orientations among possible nonpolar orientations. Large efforts were put in the *a*-plane growth until recently. The *a*-plane direct growths onto foreign substrates were performed by MOCVD [10,11,12,13,14] and by the hydride vapor-phase epitaxy (HVPE) [15,16]. LEO was applied to reduce defect densities [10,15,17,18]. The sidewall lateral epitaxial overgrowth (SLEO) technique was introduced in MOCVD growths [19,20,21]. Despite these growth results, efforts have shifted to the *m*-plane growth. Reasons were small growth-condition windows and inferior device performances of the *a* plane, in addition to stability of the *m*-plane during growths compared with that of the *a* plane. InGaN growth seems to be more difficult on the *a* plane and tends to result in less In content than growth on the *m* plane under the same growth condition.

The *m*-plane growths were performed by MOCVD (direct growth) [19,22] and HVPE (direct growth and LEO) [15,23,24,25]. Free-standing *m*-plane GaN wafers (2 inches in diameter) were created via HVPE on (100) $LiAlO_2$ [25]. SLEO has been applied to the *m*-plane growth via MOCVD and HVPE.

Figure 1 shows scanning electron microscope (SEM) images showing the evolution of *m*-plane GaN SLEO layers via MOCVD. The *m*-plane of SiC is commonly used as substrate because of its robustness in the growth atmosphere. Stripes of template GaN layers are typically made to be parallel to the *a* direction. SiO_2 and SiN_x can be used equally as SLEO masks in MOCVD growths, while they seem to create differences in HVPE growths. It is seen in Fig. 1(a) that the grown wings widely extended towards the + *c* direction (to the right in the figure) and less towards the – *c* direction; the profile can depend on growth temperature and pressure. The Ga face is hardly exposed during MOCVD growths, while the N face is typically stable until the coalescence. Competing *a*-plane facets do not appear. The vertical thickness of this stage was 4-6 microns after 210 minutes at 1180°C and 70 torr. Low pressure is commonly preferred. Low V/III ratio is essential. After coalescence, vertical growths are typically performed by increasing growth rates [Fig. 1(b)].

Figure 2 shows the coalesced surface (5 × 5 μm^2 area) observed by an atomic force microscope (AFM). Atomic steps are clearly seen. Root-mean-square (RMS) roughness was 1.15 nm, which was improved from 13.8 nm of the template layers. X-ray diffraction (XRD) was performed on these films. Full-width at half maximum (FWHM) values of *m*-plane reflection rocking curves were 0.137° and 0.408° for the beam incidence parallel to the *c* plane and to the *a* plane, respectively. Those measured on the template films were 0.198° and 2.589°, thus improvement in film quality was confirmed.

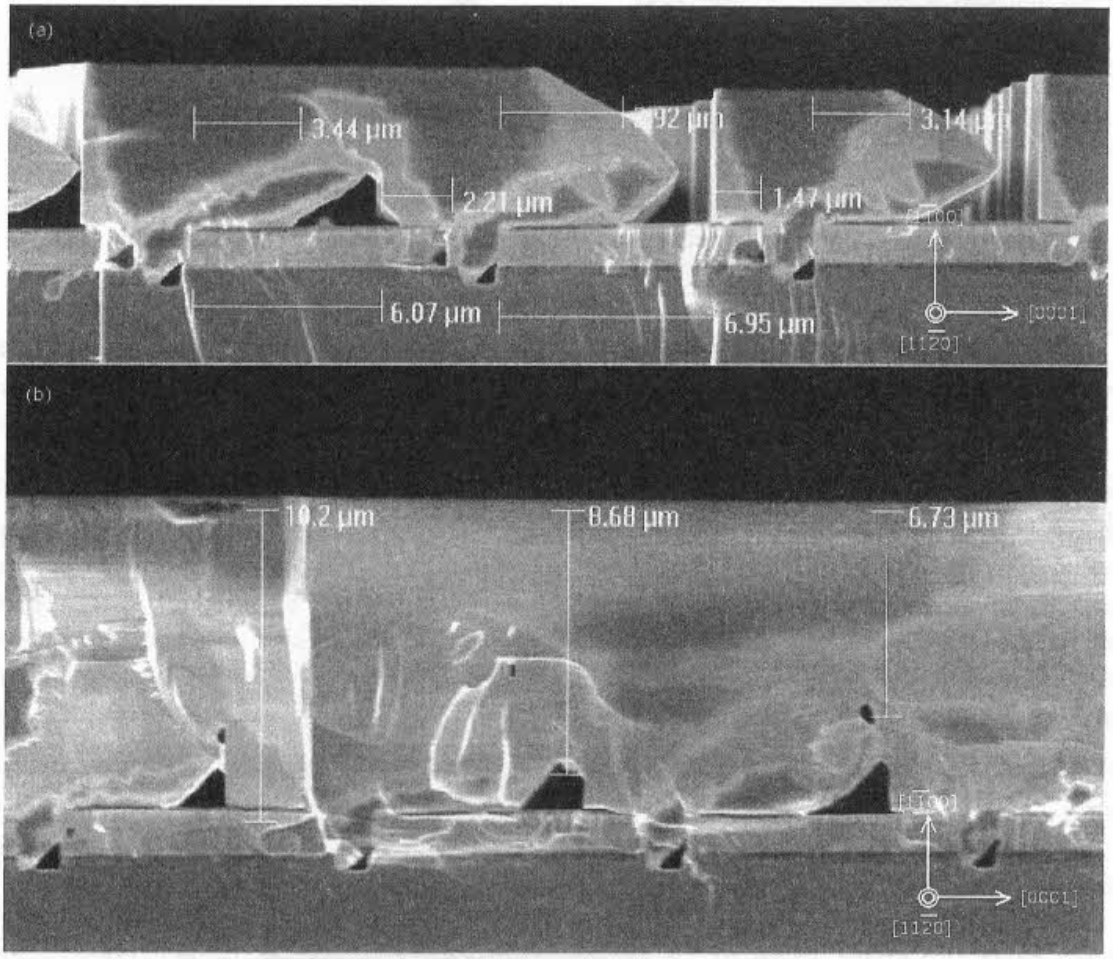

Fig. 1. SEM images showing evolution of *m*-plane GaN SLEO layers via MOCVD: (a) before and (b) after coalescence. Template GaN stripes are parallel to the *a* axis. Note that wings extend largely towards the + *c* direction. The N face is typically stable until the coalescence, while the Ga face does not show.

Figure 3 shows cross-sectional TEM images with different **g** vectors. A part of the threading dislocations has pure screw components. Threading dislocation densities were reduced from 5 × 10^9 to 3 × 10^8 cm^{-2} via SLEO. A typical threading dislocation density is in the 10^6 cm^{-2} range in the wing region. Stacking faults are somewhat problematic. Their densities were reduced from 8 × 10^5 to 4 × 10^4 cm^{-1}, yet still significantly high.

A nanomasking technique is used as an alternate approach. A Ti metal layer was deposited on the MBE template and nano-holes were created by Ti-nitridation under NH_3/H_2 gas mixture. These holes function as nucleation windows and the brittle mask-film interface occasionally allowed spontaneous film delamination. Figure 4 shows the surface and cross section of a grown *m*-plane

film. Reductions by about two orders of magnitude in threading dislocation density and by one third in stacking fault density have been confirmed on *m*-plane films via TiN_x nanomasking.

Although we have not grown LED structures on the SLEO templates, LED structure growths on LEO templates have been reported by Senda et al. [26].

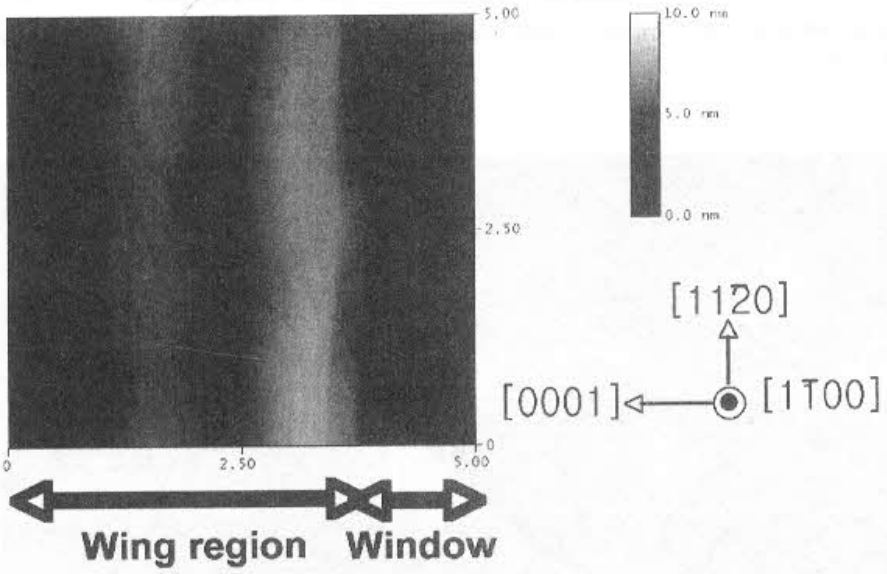

Fig. 2. An AFM image (5×5 μm^2) of the coalesced surface of a SLEO *m*-plane film. Atomic steps are clearly seen in the wing region. RMS roughness was 1.15 nm.

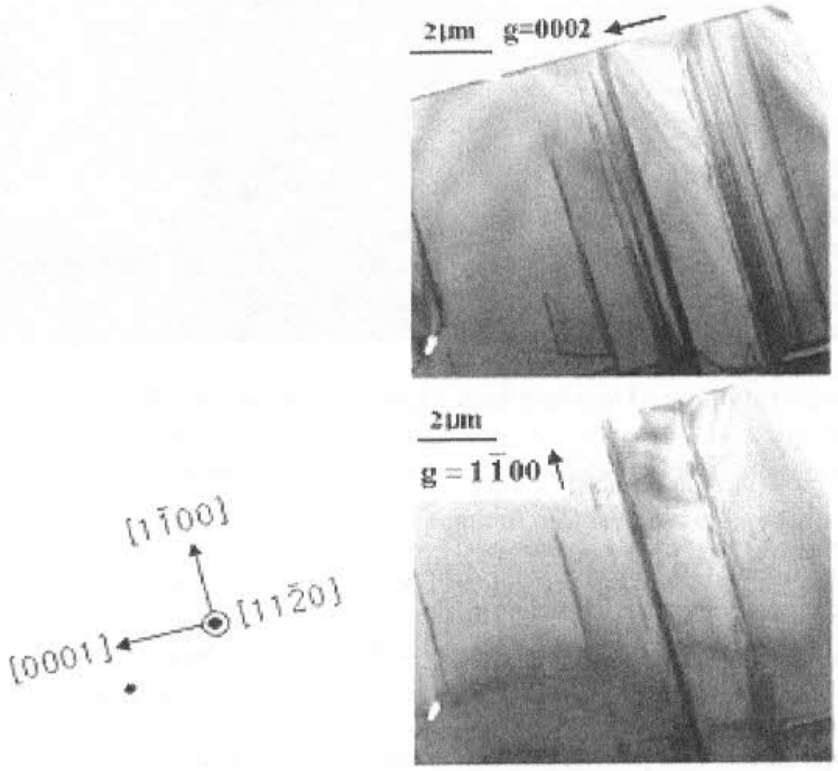

Fig. 3. Cross sectional TEM images of an SLEO *m*-plane film. The two images show the same area of the film with different **g** vectors: the top one shows threading dislocations and the bottom one shows stacking faults.

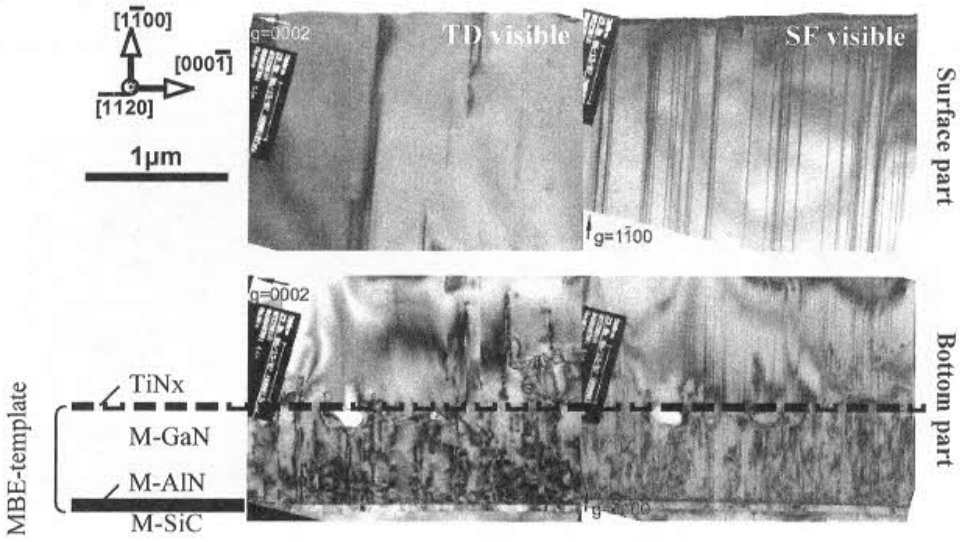

Fig. 4. Cross-section TEM images of m-plane GaN films overgrown on a TiN_x nano-mask. The estimated densities of threading dislocations (with the *c* component) and SFs at the surface were 1×10^8 cm^{-2} and 1×10^5 cm^{-1}, respectively.

Semipolar Orientations. The growth in semipolar orientations is an immature technology. Research has approached the problem in two ways: theoretical studies on optical characteristics and advantages as a function of the angle of inclination [27,28] and growth experiments to seek potential film orientations to grow on foreign substrates. LED structures are then grown on available substrates (in addition to sliced bulk-GaN substrates) to examine potential performances of those semipolar planes. The $(1\bar{1}\bar{2}2)$ orientation has exhibited promising performances in terms of In incorporation [29,30,31]. The $(10\bar{1}\bar{1})$ orientation has demonstrated performances in terms of optical output power and lasing [32,33], although those devices were mostly grown on sliced bulk-GaN substrates.

Direct growths of planar films in three semipolar orientations have been demonstrated via HVPE [8,34,35]. LEO has been applied to one of those planes [34].

Wafer off-axis cuts are strongly beneficial when films are grown on spinel substrates. Multiple domains tend to grow on on-axis substrates (no intentional off-cuts); one preferred domain can be chosen by off-cut. Figure 5 shows the off-cut effect on $(10\bar{1}\bar{1})$ films. Two domains rotated by 90° (but no twinning domains) were confirmed on an on-axis substrate [Fig. 5(a)]. Single-domain films were obtained on substrates that were off-cut towards $[011]$, which was the same direction as $[0001]$ of grown GaN films [Fig. 5(b)]. Figure 6 shows the film surface; the coalesced surface was planar [Fig. 6(a)]. The morphology observed by AFM [Fig. 6(b)] revealed the existence of stacking faults. RMS roughness resulted in 5.5 nm.

Figure 7 shows an SEM image taken at an early stage of a $(10\bar{1}\bar{3})$ film growth on a spinel on-axis substrate. Twinning domains are seen. One of twinning domains was suppressed by a substrate off-cut towards $[0001]$ of epitaxial GaN layers. Figure 8 shows the film surface; the coalesced surface was planar [Fig. 8(a)]. The morphology observed by AFM [Fig. 8(b)] revealed the existence of stacking faults. The RMS roughness resulted in 3.5 nm.

In cases where sapphire substrates were used, multiple domains did not seem to appear in epitaxial GaN layers. Figure 9 shows surface morphology of a $(10\bar{1}3)$ GaN film grown on *m*-plane sapphire. Arrow-like morphology towards GaN $[000\bar{1}]$ overlays stacking-fault morphology.

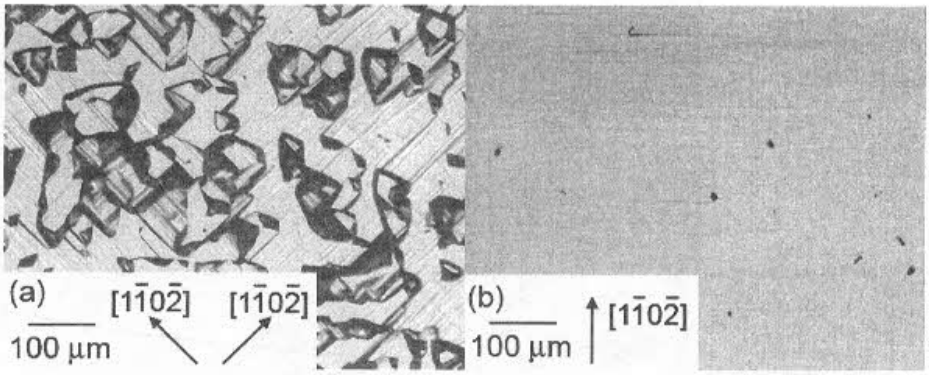

Fig. 5. Nomarski surface images of $(10\bar{1}\bar{1})$ oriented GaN films grown on (100) spinel substrates (a) without an off-cut and (b) with an off-cut towards [011].

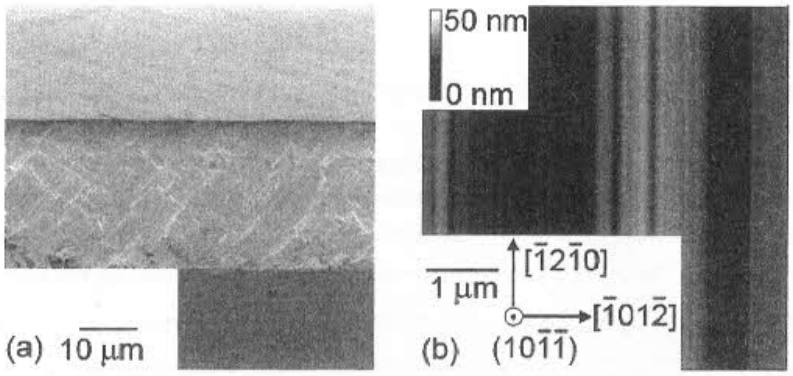

Fig. 6. Coalesced $(10\bar{1}\bar{1})$ film surface observed (a) by SEM (with a cleaved cross section shown) and (b) by AFM. RMS roughness was 5.5 nm.

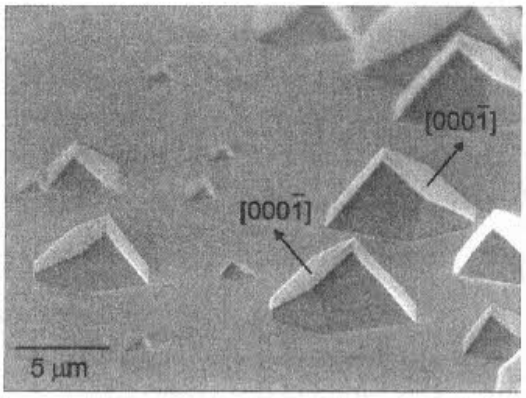

Fig. 7. An SEM image taken at an early stage of $(10\bar{1}3)$ oriented GaN growth on a (110) spinel on-axis substrate. Twinning domains are seen.

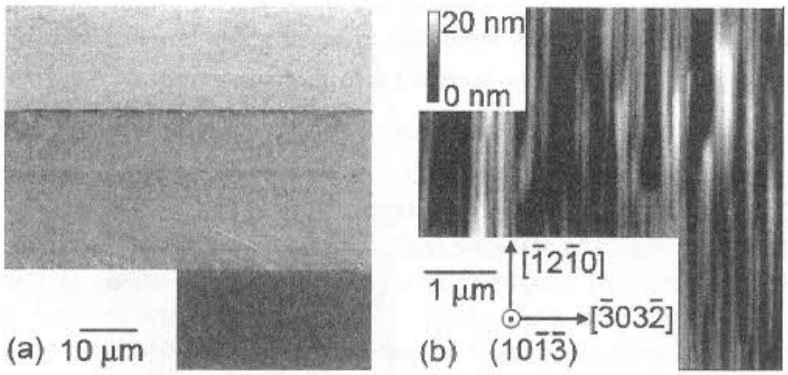

Fig. 8. Coalesced $(10\bar{1}3)$ film surface observed (a) by SEM (with a cleaved cross section shown) and (b) by AFM. The RMS roughness was 3.5 nm.

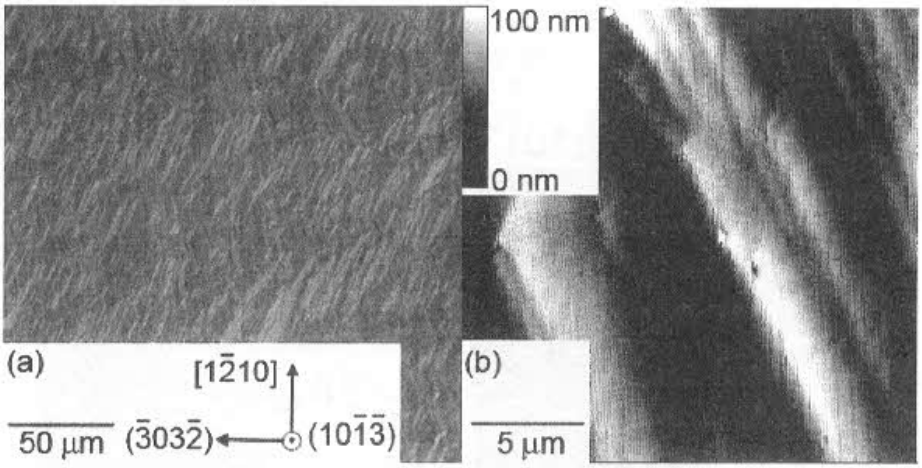

Fig. 9. Coalesced $(10\bar{1}3)$ film surface observed (a) by an optical microscope and (b) by AFM. RMS roughness was 6.5 nm. Arrow-like morphology is clearly seen in (a).

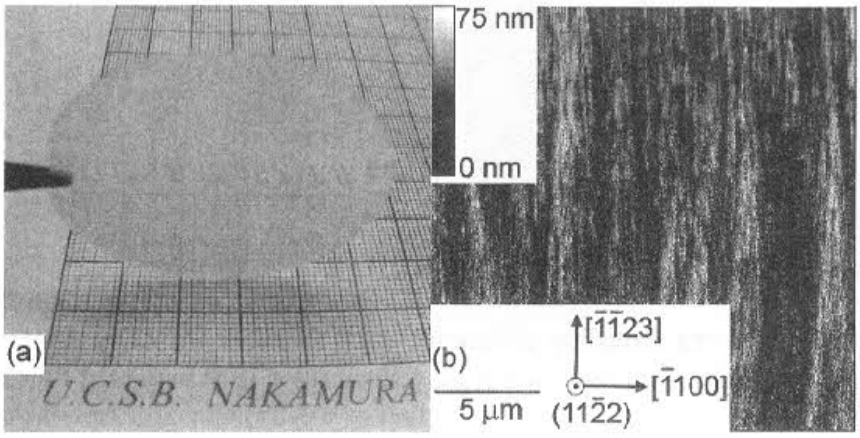

Fig. 10. $(11\bar{2}2)$ film growth on *m*-plane sapphire: (a) a two-inch wafer and (b) film surface observed by AFM. The RMS roughness was 8.4 nm.

Specular $(1\bar{1}22)$ films were obtained on *m*-plane sapphire substrates. Figure 10(a) shows a two-inch wafer. The surface was featureless and did not show stacking-fault morphology as indicated by AFM [Fig. 10(b)]. RMS roughness appeared to be slightly large; this was probably because there was a stripe morphology that may be related to microfaceting on the $(10\bar{1}1)$ plane. Growth selection between $(10\bar{1}3)$ and $(1\bar{1}22)$ was controlled predominantly by nitridation of the substrate surface prior to the growth.

Extended defects in these four types of epitaxial films were investigated via TEM. A high density of threading dislocations and stacking faults commonly exists in the films.

Figure 11 is a set of TEM images showing threading dislocations in GaN films grown on spinel substrates [Fig. 11(b) is a plan view]. Figure 12 is TEM images showing threading dislocations in GaN films grown on sapphire substrates [Figs. 12(b) and 12(d) are plan view]. Threading dislocation densities are typically on the order of 10^9 cm^{-2}. It is common for all the four film orientations that threading dislocations propagate along the *m* axis of GaN. This propagation results in that threading dislocations appear orthogonal to the *c* axis.

Figure 13 is TEM images showing stacking faults in the four types of GaN films. The stacking fault appears very similar in the four films with a density of 2×10^5 cm^{-1}. The (0001) planes are displaced towards $[1\bar{1}00]$.

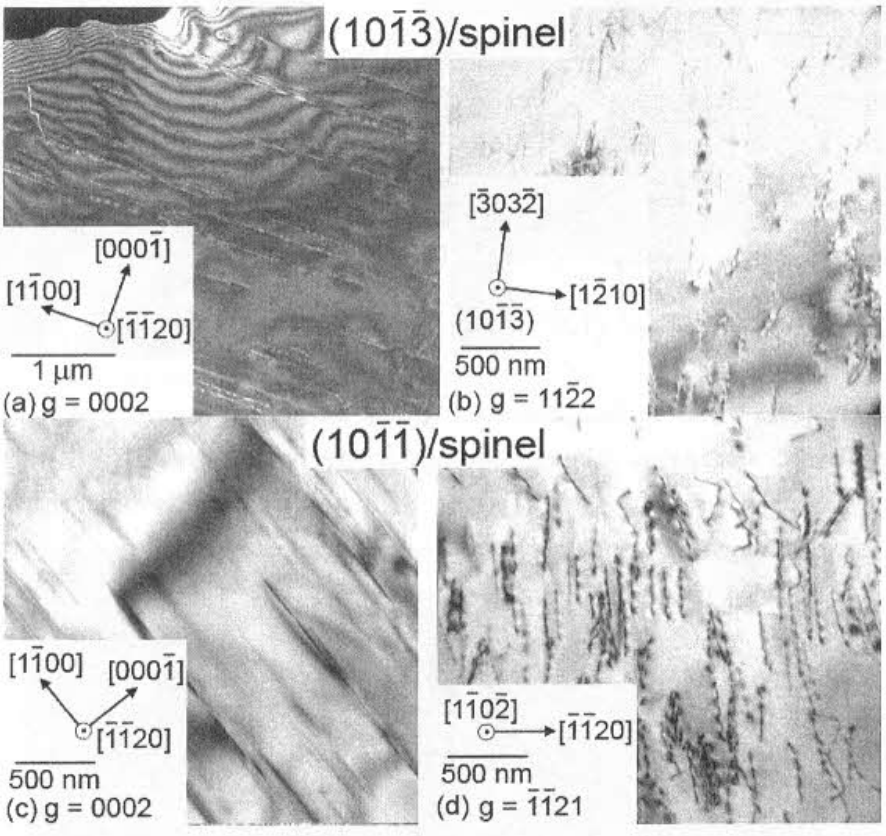

Fig. 11. TEM images showing threading dislocations in GaN films grown on spinel substrates: (a) and (b) a $(10\bar{1}3)$ oriented film with two zone-axes; (c) and (d) a $(10\bar{1}1)$ oriented film with two zone-axes.

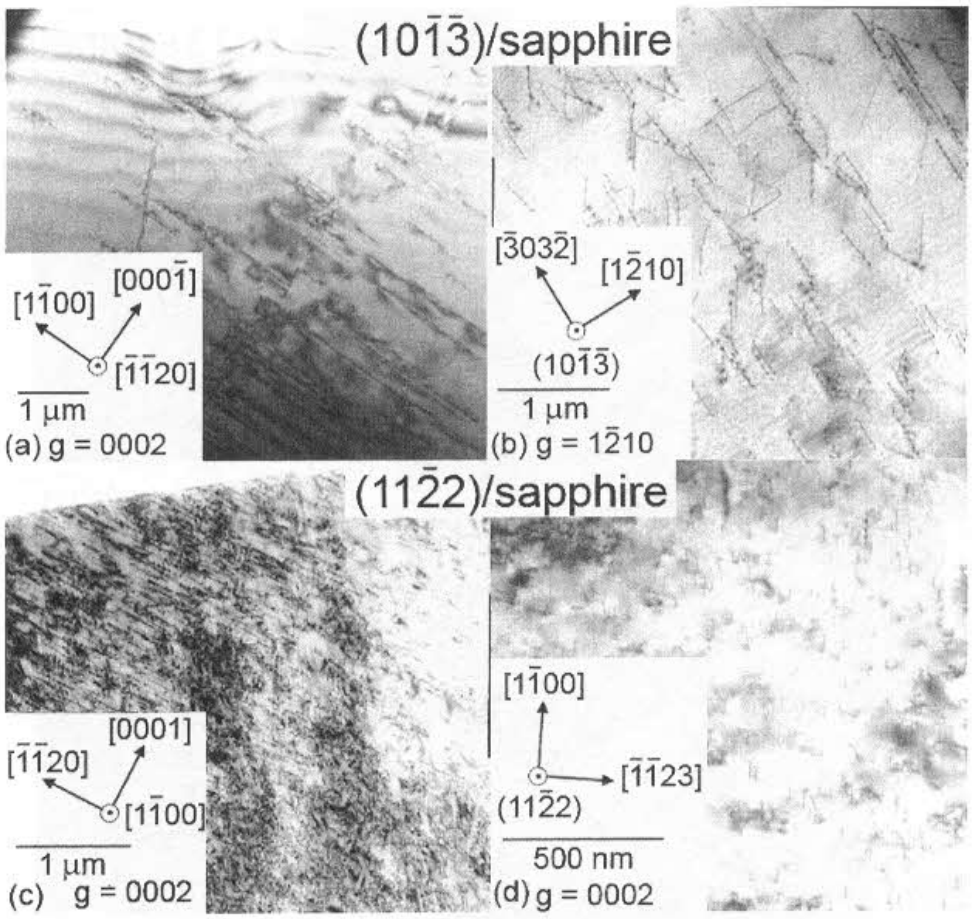

Fig. 12. TEM images showing threading dislocations in GaN films grown on sapphire substrates: (a) and (b) a $(10\bar{1}\bar{3})$ oriented film with two zone axes; (c) and (d) a $(11\bar{2}2)$ oriented film with two zone axes.

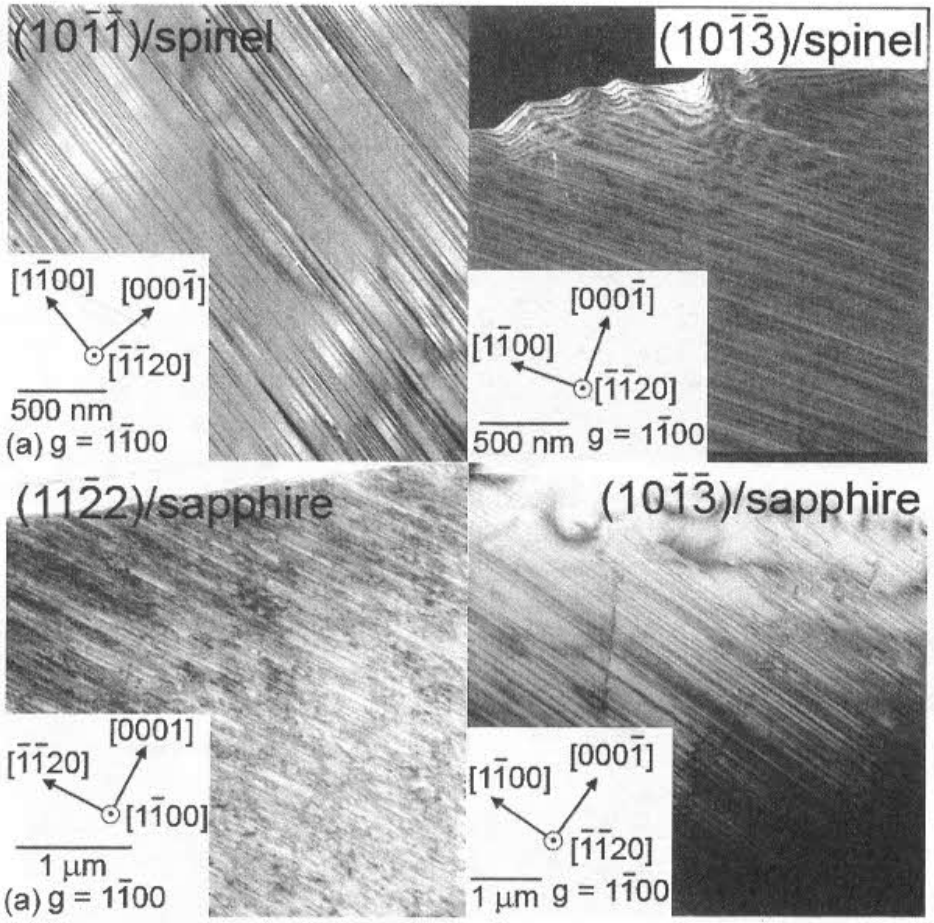

Fig. 13. Cross sectional TEM images showing stacking faults in the four types of GaN films.

In order to reduce the extended-defect densities, LEO was applied to $(1\bar{1}\bar{2}2)$ film growth. A typical stripe pattern was 15-μm wide stripes with 5-μm windows that were directed parallel to the *m* axis of the growing GaN layers. Cross sectional images of a grown film are shown in Fig. 14. Ga-face wings grew 13 μm thick, while N-face wings grew 2 μm. Formation of voids was confirmed. Voids are surrounded by $(000\bar{1})$ and $\{1\bar{1}\bar{2}2\}$ facets.

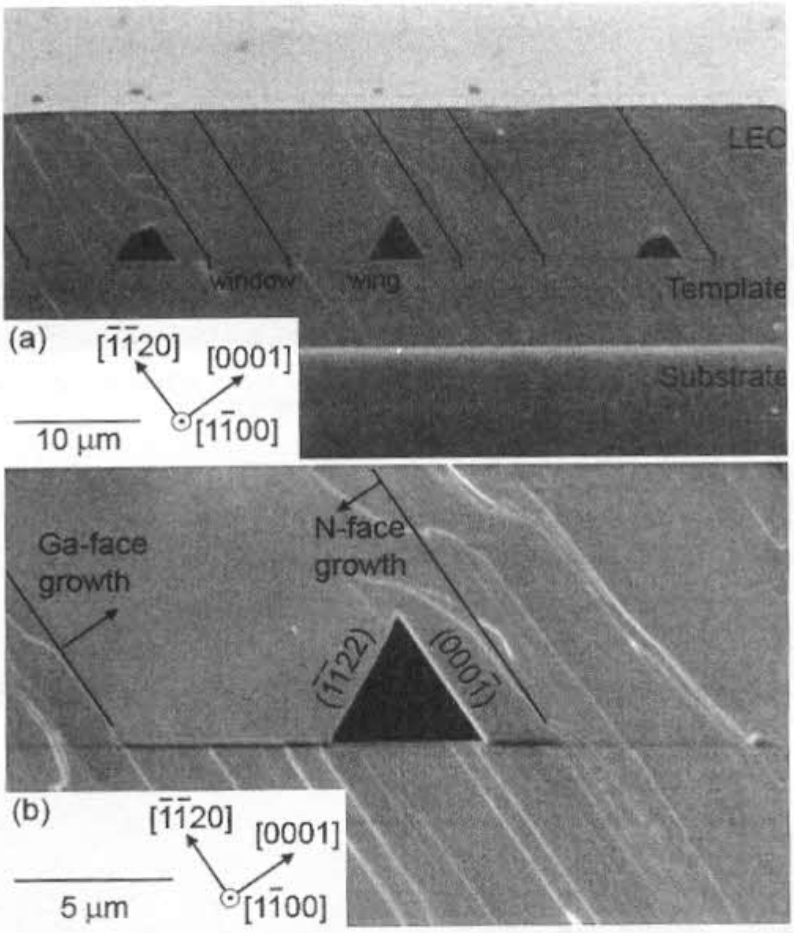

Fig. 14. Cross sectional SEM images of an LEO $(1\bar{1}22)$-oriented GaN film. Triangular dark areas are voids.

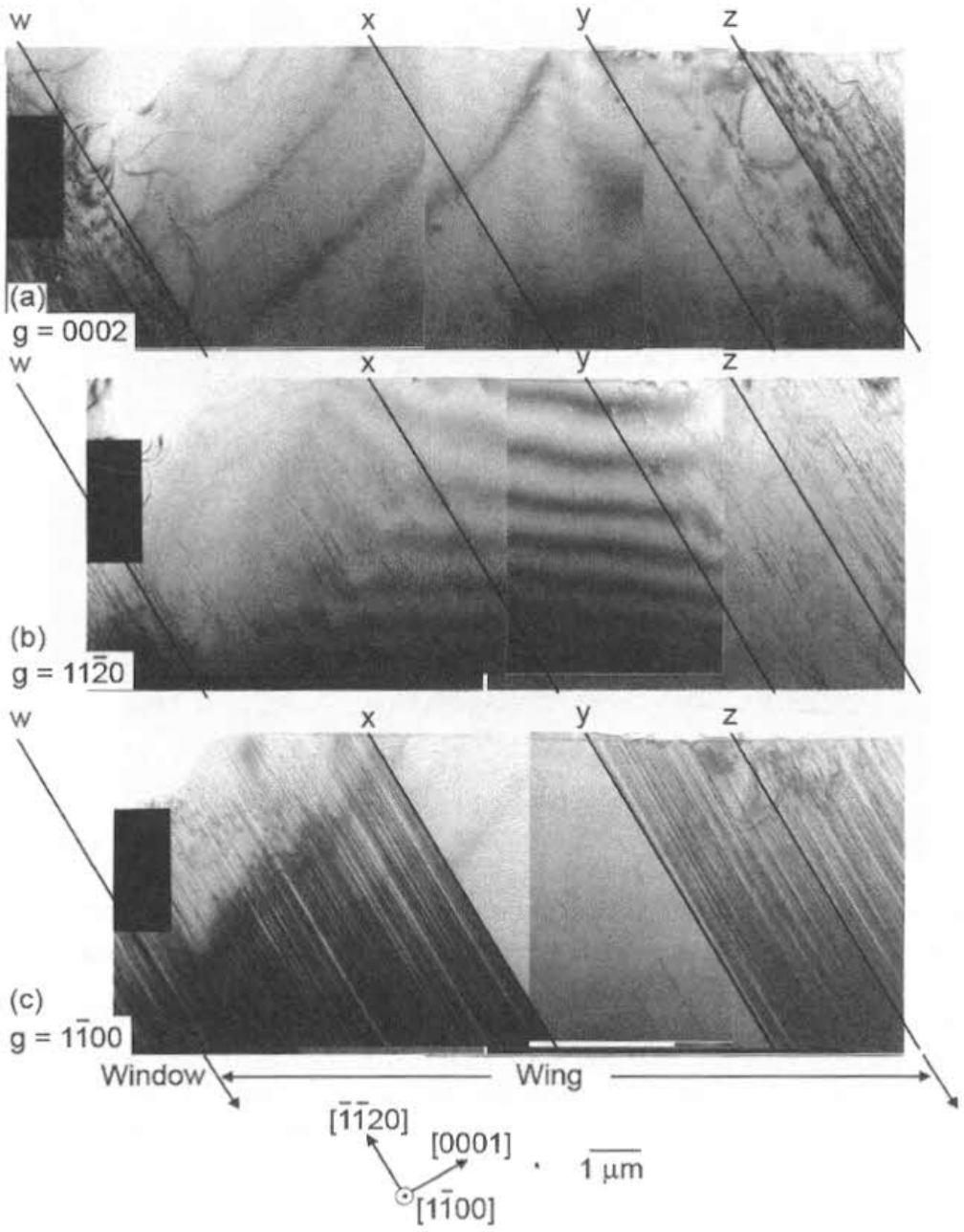

Fig. 15. Cross sectional TEM images of an LEO GaN film oriented in $(1\bar{1}\bar{2}2)$: (a) showing screw components of threading dislocations, (b) showing edge components of threading dislocations, and (c) showing stacking faults.

Figure 15 is a set of cross sectional TEM images with different **g** vectors. A significant reduction in threading dislocation densities was confirmed in the wing region. Stacking faults were reduced over the triangular voids.

Device Structure Growth

During the early stage of the nonpolar and semipolar device research, QW structures were grown on HVPE GaN templates or directly onto foreign substrates. The latest trend of using sliced bulk-GaN

substrates has revealed the potential of nonpolar and semipolar orientations as optoelectronic device fabrication planes.

Early device growth on foreign substrates. LED structures were grown by MOCVD on the *a*- and *m*-plane GaN films fabricated by HVPE [*a*: 36,37,38; *m*: 39]. Not only did the *a*-plane have narrower growth-condition windows due to its instability compared to that of the *m*-plane in the growth atmosphere, but also In incorporation into the InGaN active layer seemed to be inefficient in the *a*-plane LEDs. The *a*-plane LEDs tended to exhibit strong blue emission from non-*a*-plane facets in the structure. Since the visible spectral range was of interest as optoelectronic devices, research efforts shifted to the *m*-plane.

LED structures were grown by MOCVD on various semipolar GaN films prepared by HVPE [40,41]. Device growths directly onto foreign substrates have been performed as well on $(10\bar{1}\bar{1})$ and $(1\bar{1}\bar{2}2)$ GaN orientations [42]. A few advantages of semipolar orientations were confirmed through these early demonstrations. One was that green emission was readily achieved. Another advantage was lower forward voltages of such green LEDs than those of commercial *c*-plane LEDs.

There are attempts to utilize semipolar facets exposed during selected-area growths. Optical studies and light-emitting devices were reported by utilizing inclined facets on *c*-plane oriented substrates [43,44,45]. We have succeeded to complete LED structures with incorporation of inclined facets as the active region. Emission wavelengths ranged from blue to green with sub-mW output at 10 mA on packaged devices [46].

Device Structures on Sliced Bulk-GaN Substrates. Use of sliced bulk-GaN substrates has made a big impact and it is the mainstream of our research, nevertheless the substrate area is relatively small. Several groups have achieved high-power LEDs and LDs via MOCVD growth [*m*-plane LEDs: 47,48,49,50; *m*-plane LDs: 51,52,53,54; semipolar LEDs: 29,31,32; semipolar LDs: 33]. The *m*-plane LDs are promising to attain low threshold currents. Semipolar LEDs have a strong advantage in achieving green emission.

Device growths on *m*-plane sliced bulk-GaN substrates started based on the *c*-plane growth conditions. All growth rates appear to be very similar to those of the *c*-plane growth. The InGaN growth, however, is not trivial. The same growth condition as that of *c*-plane growths results in less In incorporation in *m*-plane films than in *c*-plane films. Incorporation of In into *m*-plane films was increased by growth optimization. We have achieved 470 nm emission from QW LEDs [47], yet not reached the green region that has been achieved by semipolar LEDs.

Because of the high-quality substrate, InGaN/GaN QW structures do not contain any threading dislocations or stacking faults as a TEM image is shown in Fig 16. Dislocation densities are estimated to be less than 1×10^4 cm^{-2}. InGaN layers are coherently strained as it can be confirmed by a reciprocal space mapping in Fig. 17.

The QW thickness seems to be optimal around 8 nm in terms of optical power output [55]. Wafer off-axis cut has been studied [56,57]. Although the mechanism has not been clearly understood yet, shallow pyramidal facets (~ 1 μm tall) were commonly formed on epitaxial film surfaces of on-axis *m*-plane layers. These facets disappeared as wafer off-cut was introduced. While wafer off-cuts towards $[000\bar{1}]$ exhibited remarkable effects on device properties [57,58], off-cuts towards $[1\bar{1}20]$ deteriorated device performances. Devices prepared on the *a* plane were significantly inferior [59].

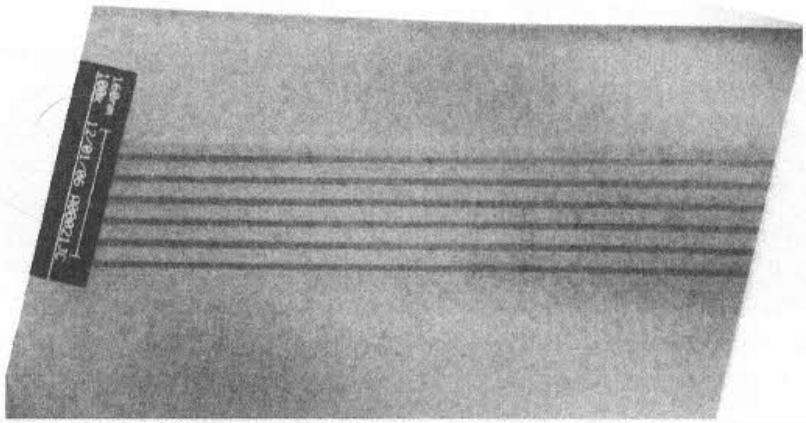

Fig. 16. A cross sectional TEM image of an InGaN/GaN QW structure fabricated on an *m*-plane sliced bulk-GaN substrate. 6 InGaN layers of 8 nm thickness are sandwiched by 18-nm-thick GaN barrier layers. An AlGaN blocking layer (~ 10 nm thick) is also seen.

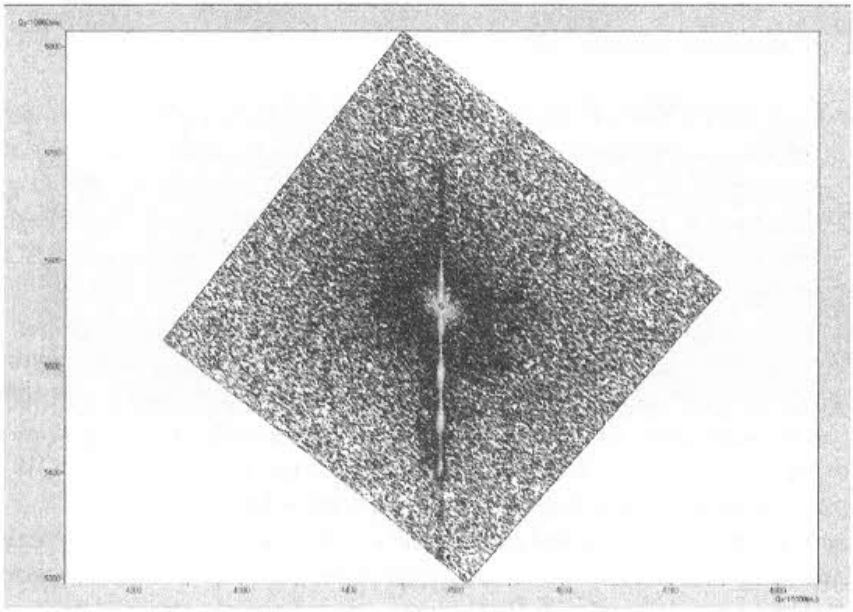

Fig. 17. A reciprocal space map of an InGaN/GaN QW structure (5 InGaN layers of 8 nm thick sandwiched by 8-nm-thick GaN layers) fabricated on an *m*-plane sliced bulk GaN substrate.

Several semipolar orientations have been examined by fabricating LED structures to evaluate their potential: $(10\bar{1}1)$, $(10\bar{1}\bar{1})$, $(10\bar{1}2)$, $(10\bar{1}\bar{2})$, $(11\bar{2}2)$, and $(11\bar{2}\bar{2})$ planes. Although growth conditions and windows are similar to those of the *c*-plane growth, the optimum condition is not necessarily the same; the $(11\bar{2}2)$ growth requires slightly lower temperatures to result in smooth surfaces, for example. Surface finish of substrates seems to have a strong effect on device growths. Figure 18 shows a TEM image of a semipolar QW structure fabricated on a sliced bulk GaN substrate [60]. No extended defects were confirmed within the observed area. Threading dislocation densities are below 1×10^7 cm^{-2}. Incorporation of In into the semipolar films is generally high compared with that of *c*-plane films. An example of XRD scan results is shown in

Fig. 19 where satellite peaks have been labeled in accordance with the EL wavelength of the device. The peak at $\omega = 18.0°$ corresponded to the EL wavelength in the present case in terms of In composition. The first-order peak at $\omega = 18.15°$ appears stronger than the zeroth-order peak; the reason is not understood yet.

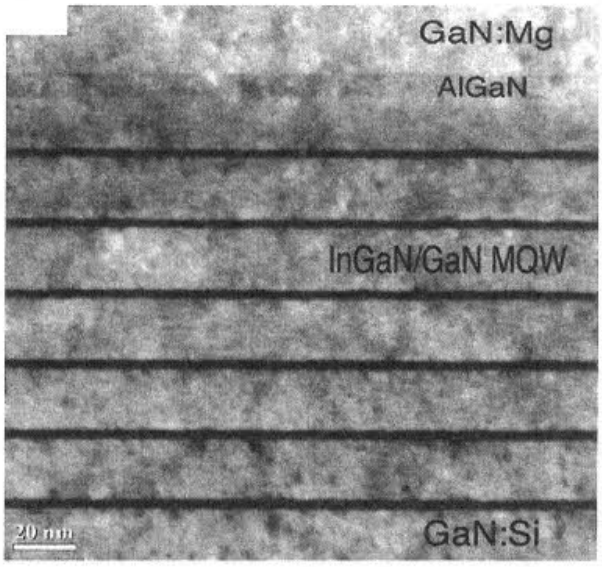

Fig. 18. A cross sectional TEM image of an InGaN/GaN QW structure fabricated in a semipolar orientation $(10\bar{1}\bar{1})$. Abrupt interfaces of six InGaN layers (3-nm thick) sandwiched by GaN barrier layers (20-nm thick) can be confirmed. An AlGaN blocking layer (10-nm thick) is also seen. The image was taken along the $[12\bar{1}0]$ zone axis in a $[12\bar{1}0]$ cross section.

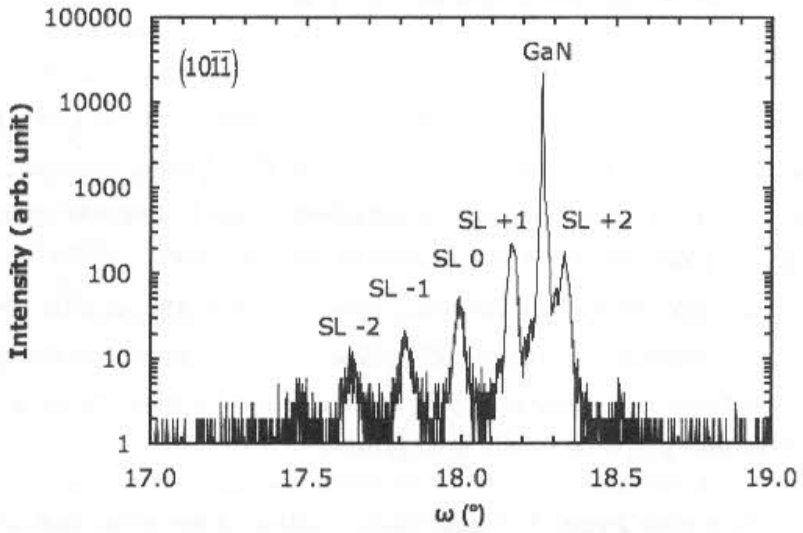

Figure 19. An XRD result of the ω-2θ scan [$(10\bar{1}\bar{1})$ reflection] on an InGaN/GaN QW structure fabricated on a $(10\bar{1}\bar{1})$ sliced bulk-GaN substrate. Satellite peaks have been labeled in accordance

with EL wavelengths of the LED. The reason why the zeroth-order peak appeared weaker than the positive first-order peak has not been understood yet.

Si (Si_2H_6) and Mg (Cp_2Mg) are used as dopants. Hall carrier concentrations of Mg-doped films are typically $p = 1 \times 10^{18}$ cm^{-3} (mobility is 17 $cm^2V^{-1}s^{-1}$), which was measured on a p^+/p double-layer structure in the $(10\bar{1}\bar{1})$ orientation. A secondary ion mass spectroscopy (SIMS) profile revealed that Mg concentrations in the double-layer structure were 1.5×10^{20} and 8×10^{18} cm^{-3}, respectively. Mg concentrations (obtained by SIMS) as a function of Cp_2Mg molar flow are presented in Fig. 20 for two semipolar orientations.

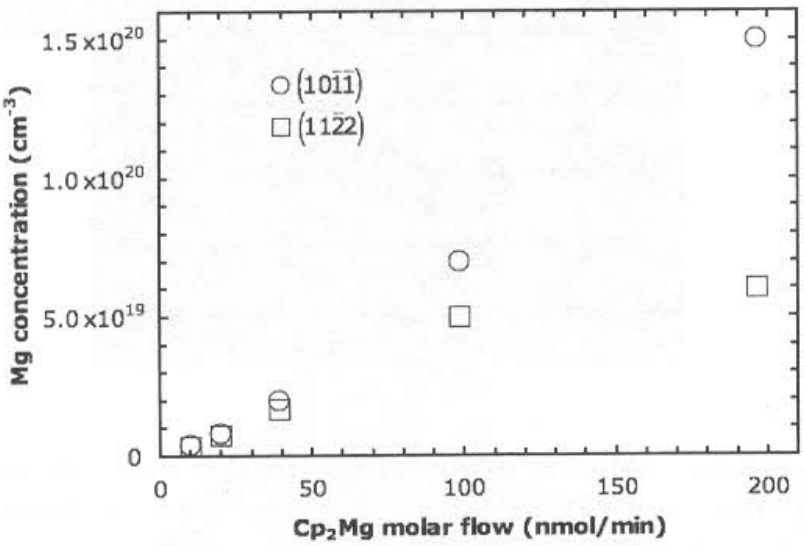

Fig. 20. Mg concentration (measured via SIMS) as a function of source-gas (Cp_2Mg) flow in $(10\bar{1}\bar{1})$- and $(11\bar{2}2)$-oriented films. Mg incorporation is reasonably linear to the source-gas flow for $(10\bar{1}\bar{1})$ and tends to saturate at high source-gas flow for $(11\bar{2}2)$.

LED results are summarized briefly as follows. LEDs prepared on the $(10\bar{1}1)$ plane were lower in radiant flux than those on the $(10\bar{1}\bar{1})$ plane. LEDs on the $(10\bar{1}\bar{1})$ plane exhibited 15-20 mW in the 400-450 nm range. Above 450 nm, optical output power tends to degrade under present growth conditions. The $(10\bar{1}2)$ plane has not been utilized in device growth. LEDs on the $(10\bar{1}\bar{2})$ plane resulted in leaky-current performances. The $(11\bar{2}2)$ plane incorporates In efficiently. Green LEDs with 9.6 mW have been fabricated on the $(11\bar{2}2)$ plane. LED structures on the $(11\bar{2}\bar{2})$ plane have appeared to be smooth films after thorough optimization. Pulsed-current lasing at 405 nm has been confirmed on LD structures prepared on the $(10\bar{1}\bar{1})$ plane.

Film Growths by Molecular Beam Epitaxy. Early studies of nonpolar and semipolar films by MBE were performed onto foreign substrates [61]. Mg doping did not generate inversion domains [62], which is often seen on *c*-oriented films. Anisotropic hole mobility in the *m* plane was observed on *m*-plane GaN films prepared on a foreign substrate [63]. Isotropic hole mobility in the *m*-plane was later confirmed on *m*-plane GaN films prepared on a sliced bulk-GaN substrate [61].

LEDs have been demonstrated via MBE [64]. Recent growth efforts are on ternary materials on sliced bulk-GaN substrates.

Below is a list of combinations of GaN (and AlN) and substrate orientations that have been demonstrated with MBE [61].

a $(11\bar{2}0)$ GaN on *r* $(10\bar{1}2)$ sapphire
m $(10\bar{1}0)$ GaN on *m* $(10\bar{1}0)$ SiC
$(10\bar{1}1)$ GaN on 4H $(10\bar{1}2)$ SiC
$(10\bar{1}3)$ GaN on 4H $(10\bar{1}6)$ SiC
$(11\bar{2}2)$ GaN on *m* $(10\bar{1}0)$ sapphire
$(10\bar{1}0)$, $(10\bar{1}2)$, and $(10\bar{1}6)$ AlN on 4H SiC

Potential Roles for Optoelectronics Applications

LEDs prepared in nonpolar orientations exhibit strongly polarized light emission [65,66]. Polarized light emitters will be a highly energy-efficient light source in applications such as liquid-crystal displays by being able to eliminate a polarizing film and color filters in the display unit. Semipolar LEDs too exhibit polarized light [30], although the degree of optical polarization is still controversial [27,58,67].

Deep-UV LEDs fabricated on the *c*-plane suffer from suppressed light emission in the surface normal direction (parallel to the *c*-axis) due to their predominant optical polarization [68,69]. Utilization of other device orientations may solve the problem.

Semipolar orientations are potential candidates for green emitters, especially the $(11\bar{2}2)$ orientation, although the mechanisms of high In incorporation on semipolar orientations are not yet well understood.

LDs fabricated in nonpolar orientations are expected to possess lower threshold currents than *c*-plane devices due to their high oscillator strengths in preferred directions [70]. Semipolar orientations may have the same advantages, although further theoretical understanding and careful geometrical designing (e.g., in cleaved-mirror implementation) are required. In semipolar QW structures, shear strain becomes nonzero [71]. Adequate calculation methods and measurement techniques need to be applied.

"Niches" for nonpolar- and semipolar-oriented devices can be summarized as follows.

I. Polarized light emission
    1) display applications
    2) light-extraction enhancement on deep-UV LEDs
    3) low-threshold LDs
II. QCSE suppression
    1) increased radiative recombination rates as In content is increased, i.e., in green emitters
    2) high power devices by increased QW thicknesses

Summary

We described developments and current status of research in nonpolar and semipolar orientations focusing on material growth. For nonpolar orientations, the *m*-plane has become the main stream of research based on highly promising device performances compared to those of devices fabricated on the *a*-plane. Semipolar orientations are still a subject of arguments in a large part. Possible semipolar orientations of planar film growths on foreign substrates are sought while effects of

utilizing semipolar orientations in optoelectronic devices are investigated experimentally and theoretically.

Sliced bulk-GaN substrates of preferred orientations became commercially available recently. Nevertheless, high-quality template materials prepared on foreign substrates are demanded for cost effectiveness. Growth techniques of nonpolar and semipolar orientations on foreign substrates are still immature. LEO-based techniques have been shown to reduce threading dislocation densities, yet are not entirely successful in reducing stacking fault densities.

A recent movement of growths of device structures and studies on their performances is to employ sliced bulk-GaN substrates. For instance, $(10\bar{1}1)$ and $(11\bar{2}2)$ planes have shown their potential in optoelectronics among possible semipolar planes. Knowledge acquired from these studies will determine the future direction and main focus of the template growth research.

Acknowledgments

The authors would like to express the acknowledgement to their coworkers for providing experimental details: Asako Hirai (nonpolar templates), Troy Baker (semipolar templates), Mathew Schmidt (nonpolar devices), Anurag Tyagi (semipolar devices), Gregor Koblmüller, and Siddarth Rajan (MBE growth). TEM was done by Feng Wu.

References

[1] M. Sumiya and S. Fuke: MRS Internet J. Nitride Semicond. Res. Vol. 9 (2004), p. 1.

[2] S. Nakamura, M. Senoh, S. Nagahama, N. Iwasa, T. Yamada, T. Matsushita, H. Kiyoku and Y. Sugimoto: Jpn. J. Appl. Phys. Vol. 35 (1996), p. L74.

[3] K. Horino, A. Kuramata, K. Domen, R. Soejima and T. Tanahashi: *Proc. Int. Symp. Blue Laser and Light Emitting Diodes* (Ohmusha, Tokyo, Japan 1996) pp. 530-533.

[4] The oral reports were made at the Electronic Materials Conference, Santa Barbara, California, June 1996 (unpublished) by H. Amano as an invited talk, and by S. Chichibu as a late news talk. Readily available published articles are: S. Chichibu, T. Azuhata, T. Sota and S. Nakamura: Appl. Phys. Lett. Vol. 69 (1996), p. 4188; T. Takeuchi, S. Sota, M. Katsuragawa, M. Komori, H. Takeuchi, H. Amano and I. Akasaki: Jpn. J. Appl. Phys. Vol. 36 (1997), p. L382.

[5] P. Waltereit, O. Brandt, A. Trampert, H.T. Grahn, J. Menniger, M. Ramsteiner, M. Reiche and K.H. Ploog: Nature (London) Vol. 406 (2000), p. 865.

[6] S.H. Park and S.L. Chuang: Phys. Rev. B vol. 59 (1999), p. 4725.

[7] T. Takeuchi, H. Amano and I. Akasaki: Jpn. J. Appl. Phys. Vol. 39 (2000), p. 413.

[8] T.J. Baker, B.A. Haskell, F. Wu, P.T. Fini, J.S. Speck and S. Nakamura: Jpn. J. Appl. Phys. Vol. 44 (2005), p. L920.

[9] A. Usui, H. Sunakawa, A. Sakai and A.A. Yamaguchi: Jpn. J. Appl. Phys. Vol. 36 (1997), p. L899.

[10] M.D. Craven: Ph.D. thesis, University of California, Santa Barbara (2003).

[11] M.D. Craven, F. Wu, A. Chakraborty, B. Imer, U.K. Mishra, S.P. DenBaars and J.S. Speck: Appl. Phys. Lett. Vol. 84 (2004), p. 1281.

[12] M.D. Craven, A. Chakraborty, B. Imer, F. Wu, S. Keller, U.K. Mishra, J.S. Speck and S.P. DenBaars: Phys. Status Solidi A Vol. 0 (2003), p. 2132.

[13] M.D. Craven, S.H. Lim, F. Wu, J.S. Speck and S.P. DenBaars: Phys. Status Solidi A Vol. 194 (2002), p. 541.

[14] M.D. Craven, S.H. Lim, F. Wu, J.S. Speck and S.P. DenBaars: Appl. Phys. Lett. Vol. 81 (2002), p. 469.

[15] B.A. Haskell: Ph.D. thesis, University of California, Santa Barbara (2005).

[16] B.A. Haskell, F. Wu, S. Matsuda, M.D. Craven, P.T. Fini, S.P. DenBaars, J.S. Speck and S. Nakamura: Appl. Phys. Lett. Vol. 83 (2003), p. 1554.

[17] M.D. Craven, S.H. Lim, F. Wu, J.S. Speck and S. P. DenBaars: Appl. Phys. Lett. Vol. 81 (2002), p. 1201.

[18] B.A. Haskell, F. Wu, M.D. Craven, S. Matsuda, P.T. Fini, T. Fujii, K. Fujito, S.P. DenBaars, J.S. Speck and S. Nakamura: Appl. Phys. Lett. Vol. 83 (2003), p. 644.

[19] B. Imer: Ph.D. thesis, University of California, Santa Barbara (2006).

[20] B. Imer, J.S. Speck and S.P. DenBaars: Appl. Phys. Lett. Vol. 88 (2006), p. 061908.

[21] B. Imer, F. Wu, J.S. Speck, S.P. DenBaars: J. Cryst. Growth Vol. 306 (2007), p. 330.

[22] B. Imer, F. Wu, M.D. Craven, J.S. Speck and S.P. DenBaars: Jpn. J. Appl. Phys. Vol. 45 (2006), p. 8644.

[23] B.A. Haskell, T.J. Baker, M.B. McLaurin, F. Wu, P.T. Fini, S.P. DenBaars, J.S. Speck and S. Nakamura: Appl. Phys. Lett. Vol. 86 (2005), p. 111917.

[24] A. Hirai, B.A. Haskell, M.B. McLaurin, F. Wu, M.C. Schmidt, K.C. Kim, T.J. Baker, S.P. DenBaars, S. Nakamura and J.S. Speck: Appl. Phys. Lett. Vol. 90 (2007), p. 121119.

[25] B.A. Haskell, A. Chakraborty, F. Wu, H. Sasano, P.T. Fini, S.P. DenBaars, J. S. Speck and S. Nakamura: J. Electron. Mater. Vol. 34 (2005), p. 357.

[26] R. Senda, A. Miura, T. Hayakawa, T. Kawashima, D. Iida, T. Nagai, M. Iwaya, S. Kamiyama, H. Amano and I. Akasaki: Jpn J. Appl. Phys. Vol. 46 (2007), L948.

[27] A.A. Yamaguchi: Jpn. J. Appl. Phys. Vol. 46 (2007), p. L789.

[28] S.-H. Park: J. Appl. Phys. Vol. 91 (2002), p. 9904.

[29] M. Funato, M. Ueda, Y. Kawakami, Y. Narukawa, T. Kosugi, M. Takahashi and T. Mukai: Jpn. J. Appl. Phys. Vol. 45 (2006), p. L659.

[30] H. Masui, T.J. Baker, M. Iza, H. Zhong, S. Nakamura and S.P. DenBaars: J. Appl. Phys. Vol. 100 (2006), p. 113109.

[31] H. Sato, A. Tyagi, H. Zhong, N. Fellows, R.B. Chung, M. Saito, K. Fujito, J.S. Speck, S.P. DenBaars and S. Nakaumura: Phys. Status Solidi RRL Vol. 1 (2007), p. 162.

[32] A. Tyagi, H. Zhong, N.N. Fellows, M. Iza, J.S. Speck, S.P. DenBaars and S. Nakamura: Jpn. J. Appl. Phys. Vol. 46 (2006), p. L129.

[33] A. Tyagi, H. Zhong, R.B. Chung, D.F. Feezell, M. Saito, K. Fujito, J.S. Speck, S.P. DenBaars and S. Nakamura: Jpn. J. Appl. Phys. Vol. 46 (2007), p. L444.

[34] T.J. Baker, Ph.D. thesis, University of California, Santa Barbara (2006).

[35] T.J. Baker, B.A. Haskell, F. Wu, J.S. Speck and S. Nakamura: Jpn. J. Appl. Phys. Vol. 45 (2006), p. L154.

[36] M.D. Craven, P. Waltereit, J.S. Speck and S.P. DenBaars: Appl. Phys. Lett. Vol. 84 (2004), p. 496.

[37] M.D. Craven, P. Waltereit, F. Wu, J.S. Speck and S.P. DenBaars: Jpn. J. Appl. Phys. Vol. 42 (2003), p. L235.

[38] A. Chakraborty, B.A. Haskell, S. Keller, J.S. Speck, S.P. DenBaars, S. Nakamura and U.K. Mishra: Appl. Phys. Lett. Vol. 85 (2004), p. 5143.

[39] A. Chakraborty, B.A. Haskell, S. Keller, J.S. Speck, S.P. DenBaars, S. Nakamura and U.K. Mishra: Jpn. J. Appl. Phys. Vol. 44 (2005), p. L173.

[40] R. Sharma, P.M. Pattison, H. Masui, R.M. Farrell, T.J. Baker, B.A. Haskell, F. Wu, S.P. DenBaars, J.S. Speck and S. Nakamura: Appl. Phys. Lett. Vol. 87 (2005), p. 231110.

[41] A. Chakraborty, T.J. Baker, B.A. Haskell, F. Wu, J.S. Speck, S.P. DenBaars, S. Namakura and U.K. Mishra: Jpn. J. Appl. Phys. Vol. 44 (2005), p. L945.

[42] J.F. Kaeding, Ph.D. thesis, University of California, Santa Barbara (2007).

[43] T. Wunderer, P. Brückner, B. Neubert, F. Scholz, M. Feneberg, F. Lipski, M. Schirra and K. Thonke: Appl. Phys. Lett. Vol. 89 (2006), p. 041121.

[44] Y. Kawakami, K. Nishizuka, D. Yamada, A. Kaneta, M. Funato, Y. Narukawa and T. Mukai: Appl. Phys. Lett. Vol. 90 (2007), p. 261912.

[45] S. Srinivasan, M. Stevens, F. A. Ponce, H. Omiya and T. Mukai: Appl. Phys. Lett. Vol. 89 (2006), p. 231908.

[46] H. Sato, H. Asamizu, H. Masui, S. Nakamura and S. P. DenBaars (unpublished).

[47] K. Iso, H. Yamada, H. Hirasawa, N. Fellows, M. Saito, K. Fujito, S.P. DenBaars, J.S. Speck and S. Nakamura: Jpn. J. Appl. Phys. Vol. 46 (2007), p. L960.

[48] K.-C. Kim , M.C. Schmidt, H. Sato, F. Wu, N. Fellows, M. Saito, J. S. Speck, S. Nakamura, S. P. DenBaars and K. Fujito: Phys. Status Solidi RRL Vol. 1 (2007), p. 125.

[49] M.C. Schmidt, K.-C. Kim, H. Sato, N. Fellows, H. Masui, S. Nakamura, S.P. DenBaars and J.S. Speck: Jpn. J. Appl. Phys. Vol. 46 (2007), p. L126.

[50] K. Okamoto, H. Ohta, D. Nakagawa, M. Sonobe, J. Ichihara and H. Takasu: Jpn. J. Appl. Phys. Vol. 45 (2006), p. L1197.

[51] R.M. Farrell, D.F. Feezell, M.C. Schmidt, D.A. Haeger, K.M. Kelchner, K. Iso, H. Yamada, M. Saito, K. Fujito, D.A. Cohen, J.S. Speck, S.P. DenBaars and S. Nakamura: Jpn. J. Appl. Phys. Vol. 46 (2007), p. L761.

[52] D.F. Feezell, M.C. Schmidt, R.M. Farrell, K.-C. Kim, M. Saito, K. Fujito, D.A. Cohen, J.S. Speck, S.P. DenBaars and S. Nakamura: Jpn. J. Appl. Phys. Vol. 46 (2007), p. L284.

[53] M.C. Schmidt, K.-C. Kim, R.M. Farrell, D.F. Feezell, D.A. Cohen, M. Saito, K. Fujito, J.S. Speck, S.P. DenBaars and S. Nakamura: Jpn. J. Appl. Phys. Vol. 46 (2007), p. L190.

[54] K. Okamoto, H. Ohta, S. F. Chichibu, J. Ichihara and H. Takasu: Jpn. J. Appl. Phys. Vol. 46 (2007), p. L187.

[55] K.-C. Kim, M.C. Schmidt, H. Sato, F. Wu, N. Fellows, Z. Jia, M. Saito, S. Nakamura, S.P. DenBaars and J.S. Speck: Appl. Phys. Lett. Vol. 91 (2007) p. 181120.

[56] A. Hirai, Z. Jia, M.C. Schmidt, R.M. Farrell, S.P. DenBaars, S. Nakamura, J.S. Speck and K. Fujito: Appl. Phys. Lett. Vol. 91 (2007), p. 191906.

[57] H. Yamada, K. Iso, M. Saito, A. Hirai, K. Fujito, S.P. DenBaars, J.S. Speck and S. Nakamura: Jpn. J. Appl. Phys. Vol. 46 (2007), p. L1117.

[58]H. Masui, H. Yamada, K. Iso, S. Nakamura and S.P. DenBaars: Appl. Phys. Lett. Vol. 92 (2008), to be published.

[59]H. Yamada, K. Iso, M. Saito, H. Hirasawa, N. Fellows, H. Masui, K. Fujito, J.S. Speck, S.P. DenBaars and S. Nakamura: Phys. Status Solidi RRL Vol. 2 (2008), p. 89.

[60] H. Zhong, A. Tyagi, N.N. Fellows, F. Wu, R.B. Chung, M. Saito, K. Fujito, J.S. Speck, S.P. DenBaars and S. Nakamura: Appl. Phys. Lett. Vol. 90 (2007), p. 233504.

[61] M.B. McLaurin: Ph. D. thesis, University of California, Santa Barbara (2007).

[62] M. McLaurin, T.E. Mates, F. Wu and J.S. Speck: J. Appl. Phys. Vol. 100 (2006), p. 063707.

[63] M. McLaurin, T.E. Mates and J. S. Speck: Appl. Phys. Lett. Vol. 86 (2005), p. 262104.

[64] P. Waltereit, H. Sato, C. Poblenz, D.S. Green, J.S. Brown, M. McLaurin, T. Katona, S.P. DenBaars, J.S. Speck, J.-H. Liang, M. Kato, H. Tamura, S. Omori and C. Funaoka: Appl. Phys. Lett. Vol. 84 (2004), p. 2748.

[65] N.F. Gardner, J.C. Kim, J.J. Wierer, Y.C. Shen and M.R. Krames: Appl. Phys. Lett. Vol. 86 (2005), p. 111101.

[66] H. Masui, A. Chakraborty, B.A. Haskell, U.K. Mishra, J.S. Speck, S. Nakamura and S.P. DenBaars: Jpn. J. Appl. Phys. Vol. 44 (2005), p. L1329.

[67] K. Kojima, M. Funato, Y. Kawakamia, S. Masui, S. Nagahama and T. Mukai: Appl. Phys. Lett. Vol. 91 (2007) 251107.

[68] K.B. Nam, J. Li, M.L. Nakarmi, J.Y. Lin and H.X. Jiang: Appl. Phys. Lett. Vol. 84 (2004), p. 5264.

[69] Y. Taniyasu, M. Kasu and T. Makimoto: Appl. Phys. Lett. Vol. 90 (2007), p. 261911.

[70] S.-H. Park: J. Appl. Phys. Vol. 93 (2003), p. 9665.

[71] A.E. Romanov, T.J. Baker, S. Nakamura and J.S. Speck: J. Appl. Phys. Vol. 100 (2006), p. 023522.